

Hepatocyte mARC1 promotes fatty liver disease

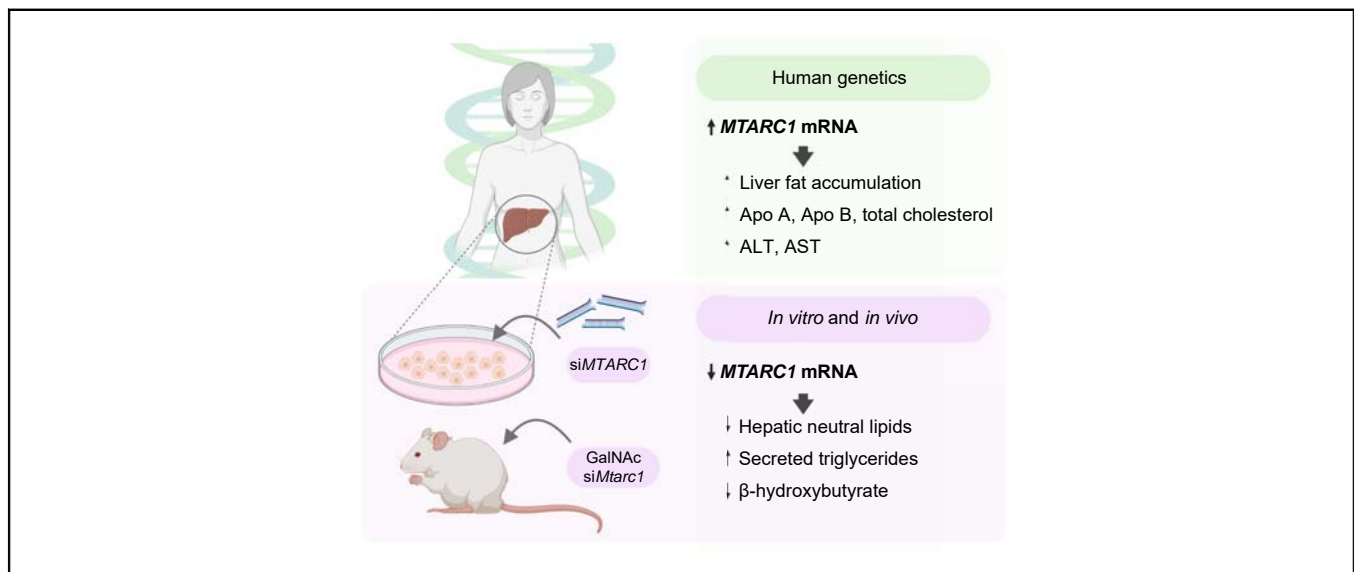
Authors

Lara C. Lewis, Lingyan Chen, L. Shahul Hameed, Robert R. Kitchen, Cyrielle Maroteau, Shilpa R. Nagarajan, Jenny Norlin, Charlotte E. Daly, Iwona Szczerbinska, Sara Toftegaard Hjuler, Rahul Patel, Eilidh J. Livingstone, Tom N. Durrant, Elisabeth Wondimu, Soumik BasuRay, Anandhakumar Chandran, Wan-Hung Lee, Sile Hu, Barak Gilboa, Megan E. Grandi, Enrique M. Toledo, Abdullah H.A. Erikat, Leanne Hodson, William G. Haynes, Natalie W. Pursell, Ken Coppieters, Jan Fleckner, Joanna M.M. Howson, Birgitte Andersen, Maxwell A. Ruby

Correspondence

lqle@novonordisk.com (L.C. Lewis), mwry@novonordisk.com (M.A. Ruby).

Graphical abstract



Highlights

- Genetically predicted increases in *MTARC1* mRNA associate with poor liver health.
- mARC1 knockdown decreases lipid accumulation in primary human hepatocytes.
- Hepatocyte-specific knockdown of mARC1 improves steatosis in a murine NASH model.

Impact and implications

We report that genetically predicted increases in *MTARC1* mRNA associate with poor liver health. Furthermore, knockdown of mARC1 reduces hepatic steatosis in primary human hepatocytes and a murine NASH model. Together, these findings further underscore the therapeutic potential of targeting hepatocyte *MTARC1* for NAFLD.



Hepatocyte mARC1 promotes fatty liver disease

Lara C. Lewis,^{1,*} Lingyan Chen,¹ L. Shahul Hameed,¹ Robert R. Kitchen,¹ Cyrielle Maroteau,¹ Shilpa R. Nagarajan,² Jenny Norlin,³ Charlotte E. Daly,¹ Iwona Szczerbinska,¹ Sara Toftegaard Hjuler,³ Rahul Patel,¹ Eilidh J. Livingstone,¹ Tom N. Durrant,¹ Elisabeth Wondimu,⁴ Soumik BasuRay,⁴ Anandhakumar Chandran,¹ Wan-Hung Lee,⁴ Sile Hu,¹ Barak Gilboa,¹ Megan E. Grandi,¹ Enrique M. Toledo,¹ Abdullah H.A. Erikat,¹ Leanne Hodson,^{2,5} William G. Haynes,¹ Natalie W. Pursell,⁴ Ken Coppieters,³ Jan Fleckner,³ Joanna M.M. Howson,¹ Birgitte Andersen,³ Maxwell A. Ruby^{1,*}

¹Novo Nordisk Research Centre Oxford, Oxford, UK; ²Oxford Centre for Diabetes, Endocrinology and Metabolism, Radcliffe Department of Medicine, University of Oxford, Churchill Hospital, Oxford, UK; ³Novo Nordisk A/S, Måløv, Denmark; ⁴Dicerna Pharmaceuticals Inc., Lexington, MA, USA; ⁵National Institute for Health Research Oxford Biomedical Research Centre, Oxford University Hospital Trusts, Oxford, UK

JHEP Reports 2023. <https://doi.org/10.1016/j.jhepr.2023.100693>

Background & Aims: Non-alcoholic fatty liver disease (NAFLD) has a prevalence of ~25% worldwide, with significant public health consequences yet few effective treatments. Human genetics can help elucidate novel biology and identify targets for new therapeutics. Genetic variants in mitochondrial amidoxime-reducing component 1 (*MTARC1*) have been associated with NAFLD and liver-related mortality; however, its pathophysiological role and the cell type(s) mediating these effects remain unclear. We aimed to investigate how *MTARC1* exerts its effects on NAFLD by integrating human genetics with *in vitro* and *in vivo* studies of mARC1 knockdown.

Methods: Analyses including multi-trait colocalisation and Mendelian randomisation were used to assess the genetic associations of *MTARC1*. In addition, we established an *in vitro* long-term primary human hepatocyte model with metabolic readouts and used the Gubra Amylin NASH (GAN)-diet non-alcoholic steatohepatitis mouse model treated with hepatocyte-specific *N*-acetylgalactosamine (GalNAc)-siRNA to understand the *in vivo* impacts of *MTARC1*.

Results: We showed that genetic variants within the *MTARC1* locus are associated with liver enzymes, liver fat, plasma lipids, and body composition, and these associations are attributable to the same causal variant (*p.A165T, rs2642438 G>A*), suggesting a shared mechanism. We demonstrated that increased *MTARC1* mRNA had an adverse effect on these traits using Mendelian randomisation, implying therapeutic inhibition of mARC1 could be beneficial. *In vitro* mARC1 knockdown decreased lipid accumulation and increased triglyceride secretion, and *in vivo* GalNAc-siRNA-mediated knockdown of mARC1 lowered hepatic but increased plasma triglycerides. We found alterations in pathways regulating lipid metabolism and decreased secretion of 3-hydroxybutyrate upon mARC1 knockdown *in vitro* and *in vivo*.

Conclusions: Collectively, our findings from human genetics, and *in vitro* and *in vivo* hepatocyte-specific mARC1 knockdown support the potential efficacy of hepatocyte-specific targeting of mARC1 for treatment of NAFLD.

Impact and implications: We report that genetically predicted increases in *MTARC1* mRNA associate with poor liver health. Furthermore, knockdown of mARC1 reduces hepatic steatosis in primary human hepatocytes and a murine NASH model. Together, these findings further underscore the therapeutic potential of targeting hepatocyte *MTARC1* for NAFLD.

© 2023 The Author(s). Published by Elsevier B.V. on behalf of European Association for the Study of the Liver (EASL). This is an open access article under the CC BY-NC-ND license (<http://creativecommons.org/licenses/by-nc-nd/4.0/>).

Introduction

Non-alcoholic fatty liver disease (NAFLD) encompasses a spectrum of histologically categorised pathologies including simple steatosis, non-alcoholic steatohepatitis (NASH), and cirrhosis.¹ Elucidating the impact of genetic variation on disease onset and progression has identified novel therapeutic targets for this major unmet medical need.² Genome-wide association studies

(GWAS) identified and validated a common missense variant (*p.A165T, rs2642438 G>A*) in mitochondrial amidoxime-reducing component 1 (*MTARC1*) that protects against all-cause cirrhosis.^{3–5} The minor A allele of *rs2642438* is associated with decreased liver fat,^{3,6} liver enzymes,^{3,7} blood cholesterol,^{3,8} and risk of NAFLD.^{9,10} A low-frequency coding variant (*p.M187K, rs17850677 T>A*) and a rare stop codon variant (*p.R200Ter, rs139321832 C>T*) in *MTARC1* are associated with lower blood cholesterol and protection from cirrhosis,³ suggesting mARC1 inhibition may have therapeutic potential for the treatment of liver disease. A slight increase in plasma triglycerides (TG) was observed in carriers of the minor A allele; however, cardiometabolic disease-based association studies of this variant in *MTARC1*^{3,8,11} do not raise any concerns for mARC1 modulation.

Keywords: Hepatic steatosis; NASH; Mendelian randomisation; Triglycerides.

Received 2 September 2022; received in revised form 19 January 2023; accepted 21 January 2023; available online 3 February 2023

* Corresponding authors. Address: Novo Nordisk Research Centre Oxford, Novo Nordisk Ltd, Innovation Building, Old Road Campus, Roosevelt Drive, OX3 7FZ, Oxford, UK. Tel.: +44-7979927835.

E-mail addresses: lqle@novonordisk.com (L.C. Lewis), mwry@novonordisk.com (M.A. Ruby).



ELSEVIER



Effects of mARC1 beyond cardiometabolic disease have not been well captured, and trait-based phenome-wide association studies may inform mARC1 biology and its associated safety profile.

The molecular function of mARC1 within NAFLD pathophysiology is unclear. mARC1 is a molybdenum-containing enzyme anchored to the outer mitochondrial membrane,^{12,13} where it catalyses the reduction of *N*-oxygenated substrates, including nitric oxide and xenobiotics,¹⁴ in combination with cytochrome b₅ type B and NADH cytochrome b₅ reductase.^{15,16} Although hepatic mARC1 expression is regulated by nutritional stimuli such as glucose deprivation, fasting and high-fat diet,¹⁷ little is known regarding the metabolic consequences of altering mARC1 levels. Depletion of mARC2, a mARC1 paralogue, decreases formation of glycerolipids in adipocytes, and mARC2 knockout mice are protected from diet-induced obesity and associated metabolic disturbances.^{18–20} As mARC1 is highly expressed in adipocytes, the sufficiency of targeting mARC1 in hepatocytes to confer the genetically predicted protective metabolic effects is unknown.

Here, we compile *in silico*, *in vitro*, and *in vivo* work to establish that hepatocyte *MTARC1* is causally associated with NAFLD. We identify novel genetic associations with body composition and liver enzymes, demonstrate a shared genetic aetiology of NAFLD-related traits at the *MTARC1* locus, and establish a causal association of genetically predicted *MTARC1* expression with these traits. mARC1 knockdown in a long-term primary human hepatocyte (PHH) system showed decreased lipid accumulation. In a murine model of NASH, we found that hepatocyte-specific mARC1 depletion decreases steatosis and markers of fibrosis. Together, this work provides the first experimental evidence that inhibition of hepatocyte mARC1 is sufficient to reduce hepatic steatosis.

Materials and methods

Please see the [Supplementary CTAT Table](#).

Genetic analyses

All analyses were performed in R v3.6.3 (R Foundation for Statistical Computing, Vienna, Austria) unless otherwise stated. Full details are provided in the [Supplementary Materials and Methods](#) and [Tables S1–S3](#).

Multi-trait colocalisation

To assess whether the genetic associations reported with metabolic traits in the region of *MTARC1* were attributable to the same underlying causal variant, statistical colocalisation using the Hypothesis Prioritisation in multi-trait Colocalisation (HyPrColoc) method was performed using priors, uniform priors, and sensitivity analyses using nonuniform priors ([Supplementary Materials and Methods](#)).

Mendelian randomisation

Two-sample Mendelian randomisation (MR) was performed to test the association of *MTARC1* mRNA expression (Genotype-Tissue Expression tissues, blood, and immune and blood cells; [Table S1](#)) with metabolic outcomes ([Table S2](#)). The two-sample MR approach (compared with one-sample MR) allowed us to use summary association statistics from two distinct studies without the need for individual participant data. See the [Supplementary Materials and Methods](#) for details.

Rare variant association tests in the UK biobank

We tested the association of rare variants in the region of *MTARC1* for association with the blood biomarkers (alanine aminotransferase [ALT], aspartate transaminase [AST], and alkaline phosphatase [ALP]) in 414,763 European ancestry participants in the UK Biobank with whole exome sequencing.²¹ Initial quality control (sex discordance, contamination, etc.) was performed by Regeneron Pharmaceuticals Inc²² and was complemented by our bioinformatic pipeline. See the [Supplementary Materials and Methods](#) for details.

PHH cell culture, siRNA transfection, and free fatty acid mixture

Cytoplastable PHH were thawed, plated, and transferred (24 h post thaw) to media containing five chemicals (5C) referred to as PHH maintenance media²³ ([Tables S4 and S5](#)). PHH were transfected on Day 8, treated with 0 or 800 μM free fatty acid (FFA) mix on Day 25, and harvested for RNA or fixed on Day 28. See the [Supplementary Materials and Methods](#) for details.

RNA extraction, cDNA synthesis, qPCR, and Western blotting

Details are provided in the [Supplementary Materials and Methods](#).

Nile red staining

The Nile red ratio was calculated as the neutral lipid fluorescence (540–15 nm/600–20 nm) divided by the phospholipid fluorescence (540–15 nm/640–20 nm).²⁴ To normalise data across experiments, non-targeting siRNA (siNT) values were set to 0% for 0 μM FFA mix and 100% for 800 μM FFA mix treatment, using the following equation: % of lipid accumulation = ((Nile Red Ratio_{gene of interest} - Nile Red Ratio_{non-targeting 0 μM FFA}) / (Nile Red Ratio_{non-targeting 800 μM FFA} - Nile Red Ratio_{non-targeting 0 μM FFA})) × 100. Details are provided in the [Supplementary Materials and Methods](#).

Supernatant assays

Conditioned media were collected from PHH in a 96-well format after 72 h in culture (0 or 800 μM FFA mix). Apolipoprotein B (apo B) content was quantified using a commercial apo B assay (Cisbio, 64APBPEH). Media concentrations of TG and FFA were measured on the AU480 chemistry analyser (Beckman Coulter; High Wycombe, UK). Metabolomic profiles were assessed using the Metabolon HD4 platform as detailed in the [Supplementary Materials and Methods](#).²⁵

In vivo mouse model

Two *in vivo* studies were carried out. Male C57BL/6J mice (n = 10–14 or n = 10–16), 5 weeks old, were fed the Gubra Amylin NASH (GAN) diet (40% fat, 22% fructose, and 2% cholesterol; D09100310, Research Diets, USA) for 44 or 36 weeks, respectively. Mice were dosed weekly s.c. for the last 8 weeks with 3 mg/kg N-acetylgalactosamine (GalNAc)-conjugated siRNA targeting murine *Mtarc1* (GalNAc-*siMtarc1*). Data were compared with a NASH vehicle control group. All animal experiments were conducted in accordance with Novo Nordisk and Gubra bioethical guidelines, which are fully compliant to internationally accepted principles for the care and use of laboratory animals. The described experiments were covered by personal licenses for Jacob Jelsing (licenses #2013-15-2934-00784 and #2017-15-0201-01215) issued by the Danish Committee for Animal Research. See the [Supplementary Materials and Methods](#) for details and [Table S6](#). Mouse plasma metabolites were analysed by MS-Omics using a Thermo Scientific

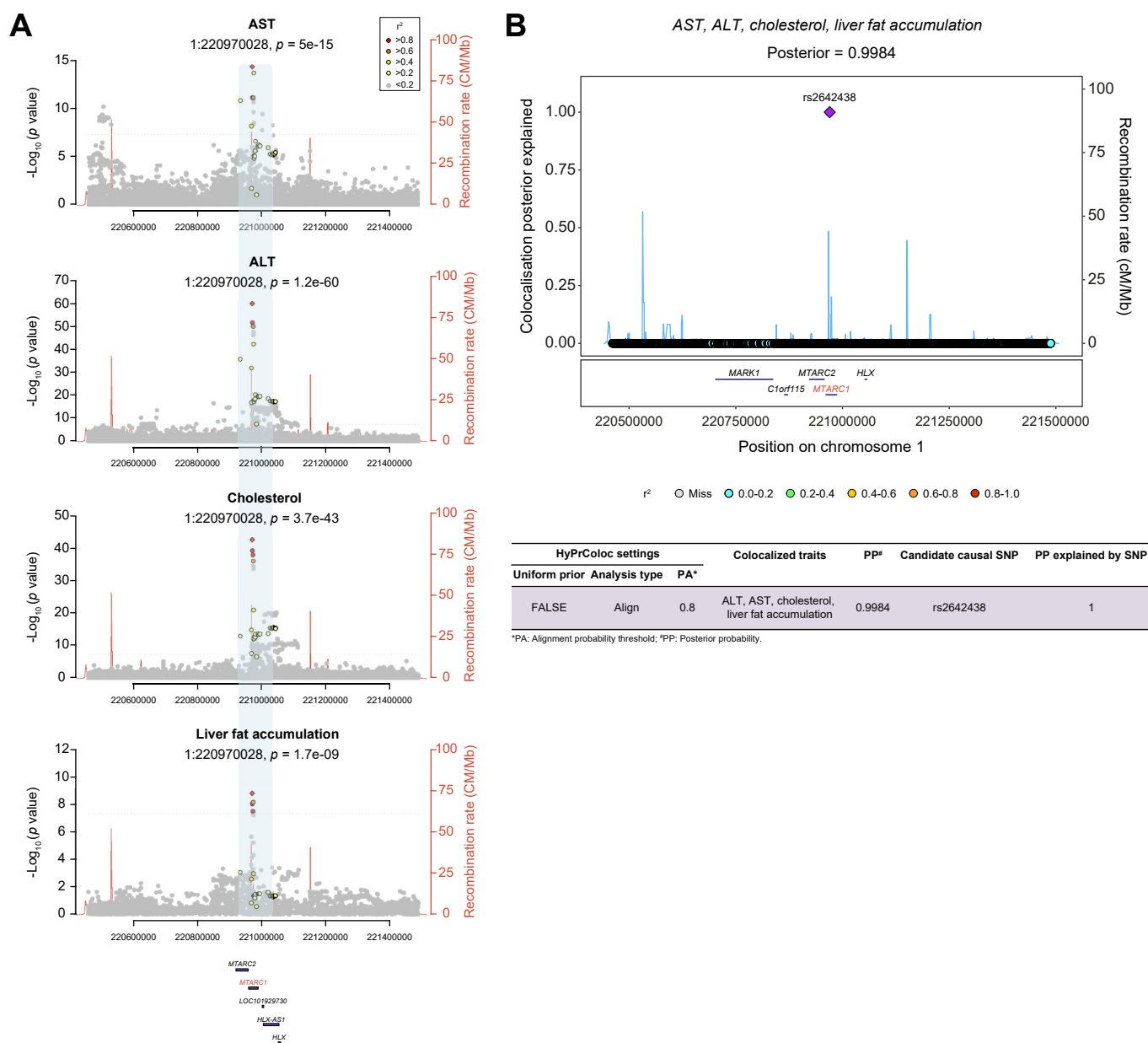


Fig. 1. Statistical colocalisation of cardiometabolic traits at the *MTARC1* locus. (A) Regional association plots at the *MTARC1* gene locus, showing the shared genetic associations with liver enzymes (ALT and AST), lipids (TC), and liver fat accumulation. Details about the statistical analysis and source of the data are given in the Materials and Methods section. Colour key indicates the correlation, r^2 , with the respective lead variants in the GWAS. (B) Plot showing the colocalisation posterior probabilities explained by each of the genetic variants at the extended *MTARC1* locus region in the colocalisation analysis. The table shows the parameters used for HyPrColoc analysis and results from HyPrColoc. ALT, alanine aminotransferase; AST, aspartate transaminase; GWAS, genome-wide association studies; *HLX*, H2.0 like homeobox; HyPrColoc, Hypothesis Prioritisation in multi-trait Colocalisation; *MARK1*, Microtubule Affinity Regulating Kinase 1; *MTARC1*, mitochondrial amidoxime-reducing component 1; TC, total cholesterol.

Vanquish LC coupled to Thermo Q Exactive HF MS. An electrospray ionisation interface was used as the ionisation source in negative and positive ionisation mode. Ultra-performance liquid chromatography was performed using a slightly modified version of a previously described protocol.²⁶

Transcriptome (mRNA) library preparation and sequencing
Details of RNA isolation, library preparation, sequencing, read quality control, and alignment for the PHH and *in vivo* samples are provided in the [Supplementary Materials and Methods](#).

Bioinformatic analyses of transcriptomic and metabolomic data

Details of the bioinformatic analyses are provided in the [Supplementary Materials and Methods](#).

Statistical analysis of *in vitro* and *in vivo* experiments

GraphPad Prism 9.0.1 was used for statistical analysis of *in vitro* experiments. For lipid accumulation and apo B in PHH, two-way ANOVA for siRNA and FFA mix conditions with Tukey's *post hoc* testing within FFA mix conditions was used. For PHH experiments

Table 1. MR estimates for the effect of genetically determined gene expression level of *MTARC1* on the metabolic traits.

Exposure	Outcome	MR causal estimate (IVW)		Heterogeneity
		Beta (SE) [†]	p value	p value [‡]
<i>MTARC1</i> gene expression (muscle)*	Alkaline phosphatase	0.0841 (0.0061)	2.96E-43	0.8102
	Alanine aminotransferase	0.0527 (0.0054)	2.08E-22	0.3087
	Aspartate aminotransferase	0.036 (0.0057)	2.03E-10	0.0011
	Direct bilirubin	0.0495 (0.0063)	6.37E-15	0.374
	Total bilirubin	0.0778 (0.006)	6.48E-38	0.0285
	SHBG	0.0306 (0.0057)	7.80E-08	0.2329
	Apolipoprotein A	0.0387 (0.0059)	6.45E-11	0.9309
	Apolipoprotein B	0.0445 (0.0059)	4.00E-14	0.1508
	Cholesterol	0.0469 (0.0057)	1.80E-16	0.9365
	LDL direct	0.045 (0.0057)	1.90E-15	0.9305
	Urate	-0.0409 (0.0095)	1.55E-05	0.3518
	Phosphate	0.0254 (0.0059)	1.41E-05	0.9591
	Liver fat accumulation	0.0648 (0.018)	4.58E-04	0.0655
	Whole-body fat-free mass	-0.021 (0.0039)	6.11E-08	0.0266
	Whole-body water mass	-0.021 (0.0039)	5.84E-08	0.0294
	Basal metabolic rate	-0.0193 (0.0041)	1.97E-06	0.0897
	Trunk fat-free mass	-0.0209 (0.0039)	8.93E-08	0.0574

Effect estimates and *p* values are provided for the IVW method. *p*-values are shown from the Cochran's Q test for heterogeneity. Full details of the results from the different MR analyses, including details of data sources and number of cases, are reported in [Tables S1, S2, S3A and B, and S9](#).

eQTL, expression quantitative trait locus; IVW, inverse-variance weighting; *MTARC1*, mitochondrial amidoxime-reducing component 1; MR, Mendelian randomisation.

* *MTARC1* gene expression in muscle is instrumented by three single nucleotide polymorphisms (cis-eQTL).

[†] Represents metabolic traits SD change per SD increase in *MTARC1* gene expression in muscle.

[‡] Heterogeneity *p* value was assessed using Cochran's Q test.

performed in a single FFA mix condition, a paired two-sided *t* test was performed. Unpaired two-sided *t* tests were used to evaluate all *in vivo* results. Significance is shown as follows: **p* ≤ 0.033, ***p* ≤ 0.002, and ****p* ≤ 0.001. No adjustment of *p* values to account for multiple comparisons has been made.

Results

Metabolic trait associations with *MTARC1* are attributable to the same genetic variants

Despite data showing associations at the *MTARC1* locus with ALT, AST, ALP, plasma LDL, total cholesterol (TC), apolipoprotein A (apo A), and apo B,³ it is unclear whether these associations are attributable to the same shared or distinct genetic causal variants and mechanisms. To address this, the HyPrColoc²⁷ method was used ([Supplementary Materials and Methods](#)). The genetic associations of liver enzymes (ALT, AST, ALP, and Sex hormone-binding globulin (SHBG)), circulating lipids (apo A, HDL cholesterol, apo B, LDL, and cholesterol), liver fat accumulation, and body composition traits (whole-body fat-free mass, whole-body water mass, trunk fat-free mass, and basal metabolic rate) identified at the *MTARC1* locus were attributable to the same genetic variant, that is, colocalised with a posterior probability of 0.80 ([Fig. 1A](#) and [Fig. S1](#)). The missense variant (p.A165T, rs2642438 G>A) explained 100% of the posterior probability, suggesting it could be the causal variant ([Fig. 1B](#)). Thus, these data provide support for a shared genetic mechanism underlying the associations of these metabolic traits at the *MTARC1* locus.

Rare and common exonic variants in *MTARC1* associate with liver phenotypes

To systemically elucidate the impact of *MTARC1* exonic variants on liver enzymes, single-variant association analysis of 270 exonic *MTARC1* variants with ALT, AST, ALP, circulating lipids, and body composition traits were performed. We replicated the association of the G allele of the common missense variant (p.A165T,

rs2642438 G>A) with increased ALT, ASP, and AST as well as with circulating lipids ([Table S7](#)). Further, we identified a novel association of a rare missense variant, rs12023067 A allele, with increased ALT ([Table S7](#)). Another rare missense variant, rs144056103, was suggestively associated with increased AST (*p* < 5 × 10⁻⁵) ([Table S7](#)). To improve statistical power to identify rare variant associations, we performed gene-based aggregate tests of rare *MTARC1* variants with liver enzymes. No significant (*p* < 1 × 10⁻⁵) effects were obtained for ALP, ALT, AST, circulating lipids, or body composition traits ([Table S8](#)).

MTARC1 gene expression associates with metabolic traits

Genetic variants associated with *MTARC1* gene expression (*i.e.* expression quantitative trait loci [eQTLs]) were used to test whether genetically determined *MTARC1* gene expression is associated with metabolic conditions. Publicly available eQTL data for *MTARC1* in 114 datasets were used, and up to three distinct eQTLs (distinct genetic variants, *r*² < 0.1, associated with *MTARC1* expression with *p* ≤ 5 × 10⁻⁸) were identified, in 16 unique tissues or cells including muscle, left ventricle of the heart, stomach, transverse colon, and rectum ([Supplementary Materials and Methods](#) and [Table S3A](#)). Importantly, most of the identified instrumental variables (IVs) are not in linkage disequilibrium with the common missense variant (p.A165T, rs2642438 G>A) and show no association with *MTARC2* gene expression ([Table S3A](#) and [S3B](#)). Analysis of these IVs showed that for every genetically predicted SD increase in *MTARC1* gene expression levels in muscle, there is an associated increase in levels of ALT, AST, ALP, apo A, apo B, TC, and liver fat accumulation, but lower levels of basal metabolic rate and whole-body fat-free mass ([Table 1](#) and [Fig. S2](#)). Similarly, genetically predicted increases in *MTARC1* gene expression level in muscle were nominally associated with increased fibrosis and cirrhosis of liver ([Table S9](#) and [Fig. S2](#)). The analyses of *MTARC1* gene expression were performed in other tissues where eQTLs were available, and consistent results were obtained in the left ventricle and rectum with those obtained in muscle ([Table S9](#)).

These results were robust to sensitivity analyses with a range of different MR approaches (Supplementary Materials and Methods). Although causal estimates from MR–Egger were less significant than those derived from the MR–inverse-variance weighting (IVW) approach, we obtained consistent effect directions of *MTARC1* gene expression on liver phenotypes (Table S9). Taken together, our analyses suggest that genetically determined increases in *MTARC1* gene expression are associated with adverse effects on liver enzymes, liver fat, and circulating lipids.

mARC1 knockdown decreases lipid accumulation and apo B secretion in PHH

To assess the impact of *MTARC1* loss of function in hepatocytes, an siRNA transfection protocol was established to knock down *MTARC1* gene expression in PHH. PHH transfected with *MTARC1* targeting siRNA (si*MTARC1*) maintained reduced *MTARC1* mRNA levels compared with siNT for 17 days (Fig. 2A). Consistent with the 12-day predicted protein half-life of mARC1 in PHH,²⁸ decreases in mARC1 protein were observed 10 days following si*MTARC1* treatment but became more pronounced on Day 17 (Fig. 2B and Fig. S3A). Protein and mRNA expression levels of mARC2 were unaffected by si*MTARC1* (Table S3B and C). The effect of si*MTARC1* and siRNA targeting Diacylglycerol O-acyltransferase 2 (*DGAT2*) (si*DGAT2*) on lipid accumulation was determined in the presence or absence of 800 μ M FFA (Fig. 2C). The siRNAs effectively reduced expression (56–86%) of their target mRNA (*DGAT2* and *MTARC1*) in 25 individual experiments using seven PHH donors (Table S10). Both si*MTARC1* and si*DGAT2* significantly reduced lipid accumulation in both conditions (Fig. 2D and E). Analysis of conditioned media from 16 experiments demonstrated that both si*MTARC1* and si*DGAT2* significantly decreased apo B secretion (Fig. 2F and Table S11). To assess the effect of mARC1 on lipid dynamics, siRNA-treated PHH were incubated with ¹³C-labelled glucose and fructose or ²H-labelled palmitate and oleate for the measurement of *de novo* lipogenesis (DNL) and fatty acid (FA) oxidation, respectively. mARC1 knockdown had no effect on DNL or FA oxidation (Fig. S4A and B). To determine whether mARC1 knockdown alters the import and export of lipids, FFA and TG concentrations were quantified in conditioned media from the above experiments. The majority of the 800 μ M FFA was taken up by the PHH, and this was unaffected by si*MTARC1* (Fig. S4C). In contrast, si*MTARC1* significantly increased the concentration of TG in conditioned media (Fig. 2G).

Hepatocyte-specific mARC1 knockdown reverses steatosis and decreases markers of fibrosis in the Gubra DIO-NASH mouse model

To determine the impact of hepatocyte-specific knockdown of *Mtarc1* on hepatic steatosis, inflammation, and fibrosis *in vivo*, a diet-induced obese (DIO)-NASH mouse model was used. Briefly, C57BL/6J mice fed a high-fat, high-fructose, high-cholesterol diet for 44 weeks were randomised based on biopsy results after 36 weeks and treated weekly with GalNac-si*Mtarc1* or PBS for an additional 8 weeks. GalNac-si*Mtarc1* effectively decreased *Mtarc1* mRNA and slightly, but significantly, also reduced *Mtarc2* mRNA (Fig. 3A and Fig. S5A). GalNac-si*Mtarc1* decreased the liver-to-body weight ratio without altering body weight (Fig. 3B and Fig. S5B). GalNac-si*Mtarc1* decreased histologically determined steatosis (Fig. 3C and Table 2). In addition, intrahepatic concentrations of TG and TC determined by extraction were decreased by GalNac-si*Mtarc1* treatment, whereas plasma TG increased and plasma TC was reduced (Fig. 3D–G). Plasma liver

enzymes (Fig. S5C and D) and metrics of hepatic inflammation were unchanged by mARC1 knockdown (Fig. S5E–H and Table 2). GalNac-si*Mtarc1* did not alter total fibrosis, as assessed by Sirius Red staining, or levels of collagen 1 but reduced hepatic α -smooth muscle actin (α -SMA) staining (Fig. 4A–C and Table 2). In addition, expression of several genes involved in fibrogenesis were downregulated by GalNac-si*Mtarc1* (Fig. 4D). Mild hepatocyte ballooning was observed in the GalNac-si*Mtarc1*-treated group (Table 2) but as glycogen accumulation can confound the quantification of hepatocyte ballooning,²⁹ measurement of hepatic glycogen was included in a second animal experiment. The majority of the effects of mARC1 knockdown on hepatic phenotypes were reproduced in the second study, including mild hepatocyte ballooning (Fig. S6A–F), and hepatic glycogen was significantly elevated in the GalNac-si*Mtarc1* group (Fig. S6G).

mARC1 knockdown results in transcriptional changes related to lipid metabolism

To determine the global transcriptional impact of *MTARC1* loss of function, RNA sequencing on PHH treated with si*MTARC1* or siNT (Supplementary Materials and Methods) was performed. In addition to *MTARC1*, si*MTARC1* altered 17 mRNAs (Fig. 5A and Table S12) enriched in processes and pathways including *response to lipid* and *lipid transport* (Table S13). Gene set enrichment analysis identified alterations in lipid and FA metabolic processes and the peroxisome proliferator-activated receptor (PPAR) signalling pathway (Fig. S7A and Table S14). RNA sequencing of the liver of the GalNac-si*Mtarc1*-treated DIO-NASH mice revealed over 600 differentially expressed protein coding genes (Supplementary Materials and Methods and Table S15) compared with vehicle-treated mice. Although there was no overlap with regulated mRNAs in PHH (except *Mtarc1*), effects of GalNac-si*Mtarc1* on genes involved in the PPAR signalling and lipid metabolism were observed (Fig. S7B, Table S16 and S17).

mARC1 regulates the Kennedy pathway and 3-hydroxybutyrate

To gain insight into the metabolic impact of mARC1 knockdown, metabolomic analysis on conditioned media from PHH treated with either si*MTARC1* or siNT was performed. Knockdown of mARC1 affected the abundance of 47 metabolites, including increases in *O*-phosphoethanolamine and phosphocholine, and a decrease in 3-hydroxybutyrate (Fig. 5B and Table S18). A network analysis of putative interacting proteins of the metabolites significantly altered by si*MTARC1* identified enrichments in the *Kennedy pathway from sphingolipids* (WP3933, false discovery rate [FDR] = 0.01) and *One-carbon metabolism and related pathways* (WP3940, FDR = 0.04) (Fig. 5C). To test if hepatocyte-specific *Mtarc1* knockdown was sufficient to impact metabolite concentration in the circulatory system of a whole organism, metabolites in plasma from mice treated with GalNac-si*Mtarc1* were profiled. Thirteen of the 47 *MTARC1*-affected metabolites identified in our PHH samples were also identified in mice (Methods and Table S19). Of these, only 3-hydroxybutyrate was altered in GalNac-si*Mtarc1* animals (Fig. 5B and Table S20).

Discussion

Using a combination of genetic approaches and experimental manipulations, a causal relationship between mARC1 expression and liver enzymes, plasma lipids, and liver fat has been

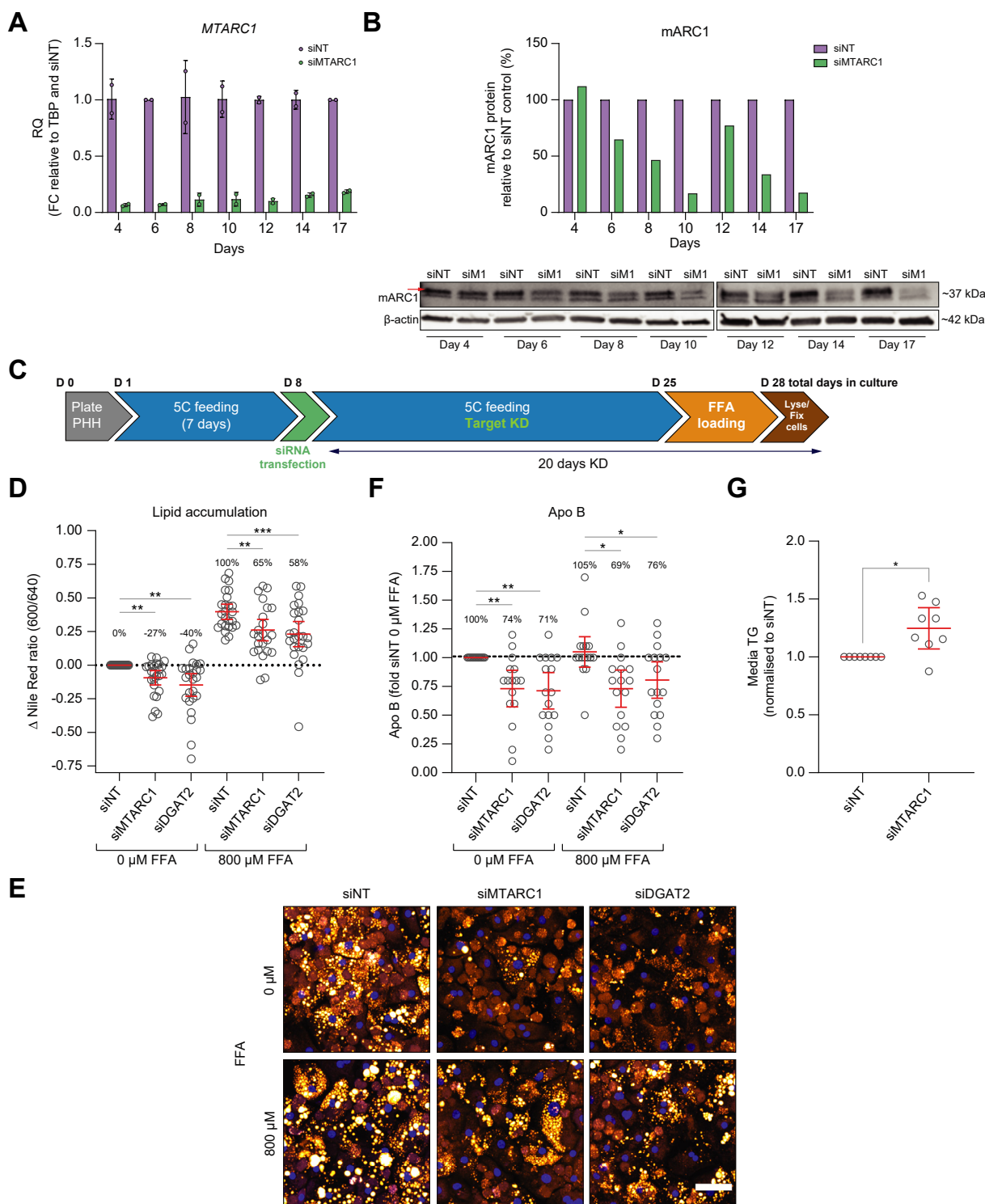


Fig. 2. mARC1 knockdown decreases lipid accumulation and apo B secretion in PHH. Validation of (A) mRNA and (B) protein levels following *MTARC1* siRNA knockdown in PHH over 17 days. (C) Workflow for culturing of PHH, siRNA transfection, and endpoint collections. (D) Lipid accumulation data following siRNA-mediated knockdown of *MTARC1* and *DGAT2* relative to NT siRNA, n = 25 independent experiments. (E) siRNA knockdown of *MTARC1* and *DGAT2* reduces lipid accumulation with and without FFA mix loading in PHH. Fluorescence images of nuclei (blue) and lipid droplets (hot) from siRNA knockdown PHH treated with FFA mix. Scale bar: 50 μ m. (F) Reduced apo B expression observed following knockdown with *MTARC1* siRNA relative to NT siRNA, n = 16 independent experiments. (G) Increased media TG levels observed following knockdown with *MTARC1* siRNA relative to NT siRNA, n = 8 independent experiments. Data are presented as mean \pm 95% CI, * p \leq 0.033, ** p \leq 0.002, *** p \leq 0.001 (D and F, two-way ANOVA with Tukey's *post hoc* testing within FFA mix conditions; G, paired *t* test). 5C, five chemicals; apo B, apolipoprotein B; FC, fold change; FFA, free fatty acid; KD, knockdown; *MTARC1*, mitochondrial amidoxime-reducing component 1; NT, non-targeting; PHH, primary human hepatocytes; RQ, relative quantification; siDGAT2, siRNA targeting *DGAT2*; siMTARC1, *MTARC1* targeting siRNA; TBP, TATA-box binding protein; TG, triglycerides.

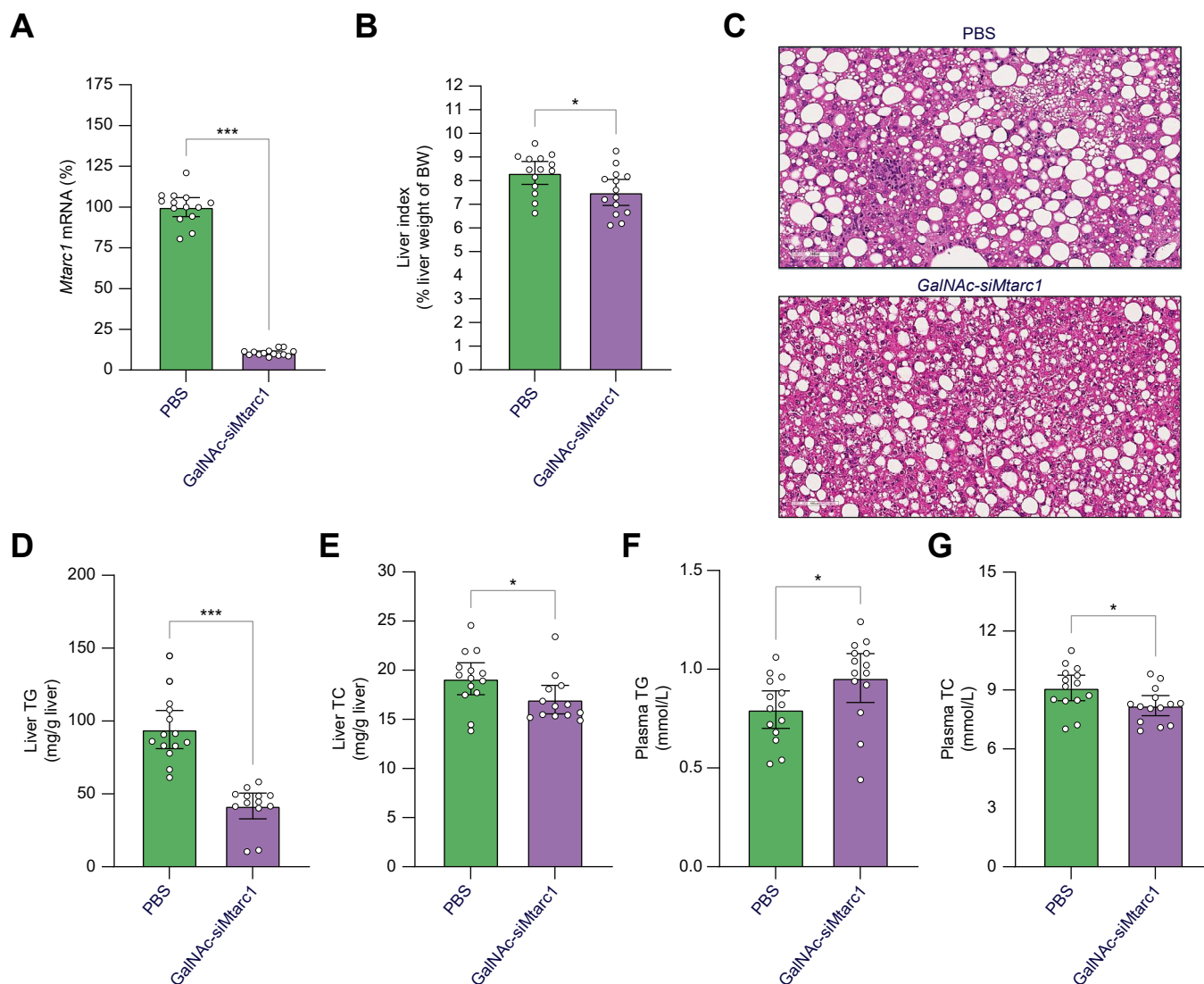


Fig. 3. Hepatocyte-specific *Mtar1* knockdown reverses steatosis in a DIO-NASH mouse model. C57BL/6J mice fed a high-fat, high-fructose, high-cholesterol diet for 44 weeks were randomised based on biopsy results and treated weekly with a GalNAc-*siMtar1* or PBS for 8 weeks. (A) mRNA expression for *Mtar1*. (B) % Liver weight of BW. (C) Liver TG as mg/g of liver. (D) Liver TC as mg/g of liver. (E) Plasma TG (mmol/L). (F) Plasma TC (mmol/L). Data are presented as mean \pm 95% CI, n = 10–14, * $p \leq 0.033$, *** $p \leq 0.001$ (unpaired *t* test). BW, body weight; GalNAc, N-acetylgalactosamine; GalNAc-*siMtar1*, GalNAc-conjugated siRNA targeting murine *Mtar1*; *Mtar1*, mitochondrial amidoxime-reducing component 1; NASH, non-alcoholic steatohepatitis; TC, total cholesterol; TG, triglycerides.

demonstrated. Previous genetic findings have been extended^{3,8} by establishing novel associations of rare *MTARC1* variants with liver enzymes, a shared aetiology of traits at the *MTARC1* locus, and a relationship between increased *MTARC1* mRNA and worsening of liver enzymes, apo B, and body composition. mARC1 knockdown in PHH decreases lipid content and apo B secretion. In a murine model of NASH, hepatocyte-specific mARC1 knockdown improved hepatic steatosis and decreased markers of fibrosis. Thus, although genetic variation in *MTARC1* is causally associated with a range of metabolic traits, hepatocyte-specific decreases in *MTARC1* mRNA are sufficient to recapitulate alterations in hepatic and serum lipids.

A common *MTARC1* missense variant (p.A165T, rs2642438 G>A) has been associated with all-cause cirrhosis, NAFLD, liver enzymes, and serum lipids.^{3,8} Here, HyPrColoc was applied to show that rs2642438 is the likely causal variant across these traits, demonstrating a shared genetic mechanism. In addition to

the common missense variant (p.A165T, rs2642438 G>A), we identified novel missense *MTARC1* variants associated with liver enzymes. However, as the impact of missense variants in *MTARC1* on protein levels, localisation, and activity is unclear, the directional effect of *MTARC1* can only be inferred from the rare loss of function variant encoding a premature stop codon (p.R200Ter, rs139321832:C:T).³⁰ Using MR, we demonstrated that increased *MTARC1* mRNA was associated with adverse effects on metabolic traits. Although the tissues with available eQTLs (muscle, left heart ventricle, and rectum) may not contribute to the associated phenotypes, the concordant effect direction indicates a consistent impact of the gene variants on gene expression across tissues. Our work reports a novel association of the *MTARC1* locus with body composition traits, suggesting an additional metabolic benefit of decreased mARC1 expression, and underscores how genetic variants can have diverse systemic effects likely driven by multiple organs.

Table 2. Effect of GalNac-siMtarc1 on histological scoring of livers.

	Steatosis***		Lobular inflammation		Ballooning degeneration***		Fibrosis stage	
	PBS	GalNac-siMtarc1	PBS	GalNac-siMtarc1	PBS	GalNac-siMtarc1	PBS	GalNac-siMtarc1
1-point worsening	0.00%	0.00%	0.00%	0.00%	0.00%	78.60%	0.00%	0.00%
No change	100.00%	7.10%	85.70%	57.10%	100.00%	21.40%	71.40%	71.40%
1-point improvement	0.00%	78.60%	14.30%	21.40%	0.00%	0.00%	28.60%	28.60%
2-point improvement	0.00%	14.30%	0.00%	21.40%	0.00%	0.00%	0.00%	0.00%

An unpaired t test was performed for each parameter.

****p* ≤ 0.001.

GalNac, N-acetylgalactosamine; GalNac-siMtarc1, GalNac-conjugated siRNA targeting murine *Mtarc1*; *Mtarc1*, mitochondrial amidoxime-reducing component 1.

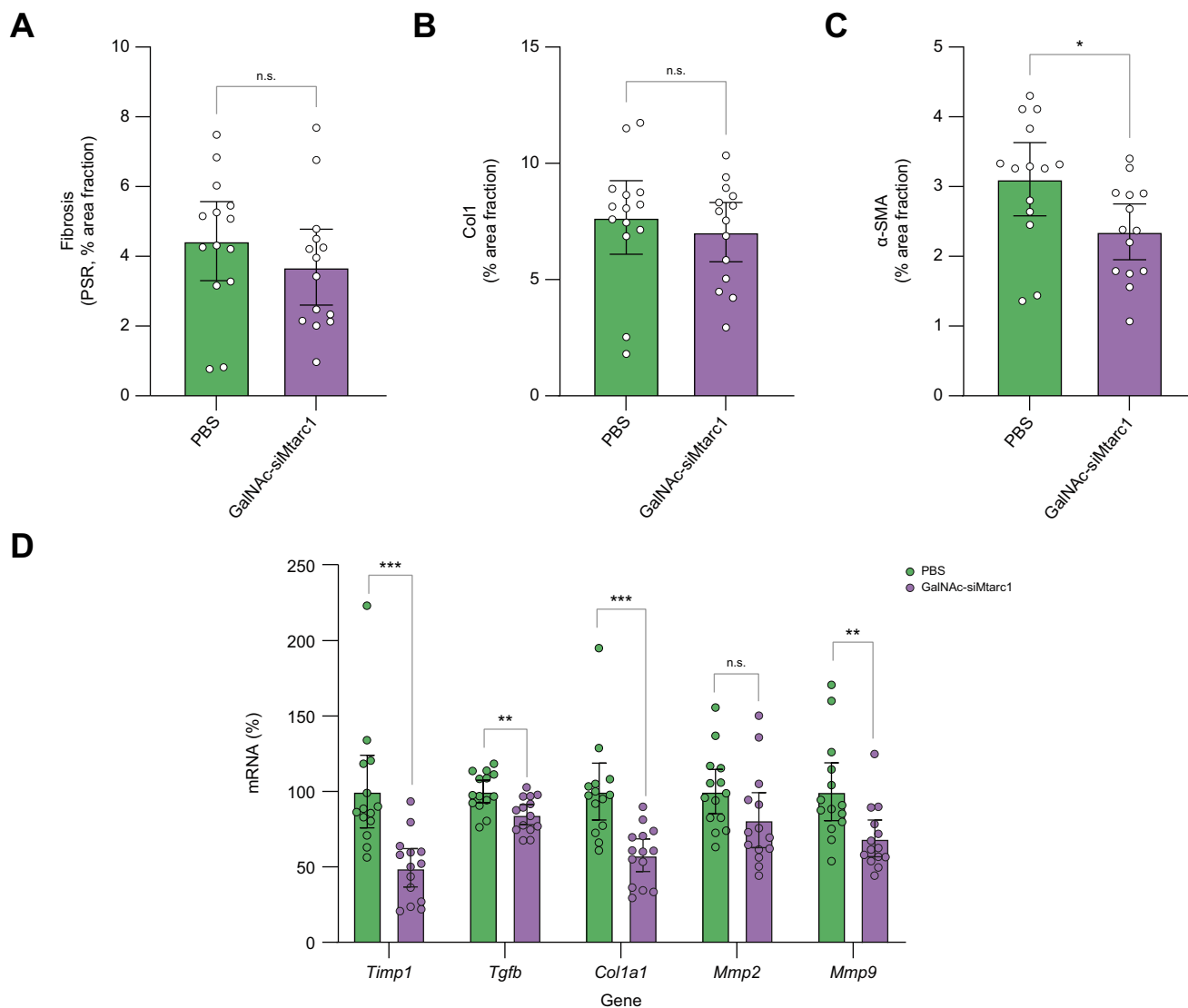


Fig. 4. Hepatocyte-specific *Mtarc1* knockdown decreases markers of fibrosis in a DIO-NASH mouse model. *C57Bl/6J*Rj mice fed a high-fat, high-fructose, high-cholesterol diet for 44 weeks were randomised based on biopsy results and treated weekly with a GalNac-siMtarc1 or PBS for 8 weeks. (A) Fibrosis as PSR, % area fraction. (B) Col1 as % area fraction. (C) α -SMA as % area fraction. (D) mRNA expression for fibrosis-associated genes; *Timp1*, *Tgfb*, *Col1a1*, *Mmp2*, and *Mmp9*. Data are presented as mean \pm 95% CI, *n* = 10–14, n.s., **p* ≤ 0.033, ***p* ≤ 0.002, ****p* ≤ 0.001 (unpaired t test). α -SMA, α -smooth muscle actin; GalNac, N-acetylgalactosamine; GalNac-siMtarc1, GalNac-conjugated siRNA targeting murine *Mtarc1*; *Mtarc1*, mitochondrial amidoxime-reducing component 1; NASH, non-alcoholic steatohepatitis; PSR, Picro-Sirius Red.

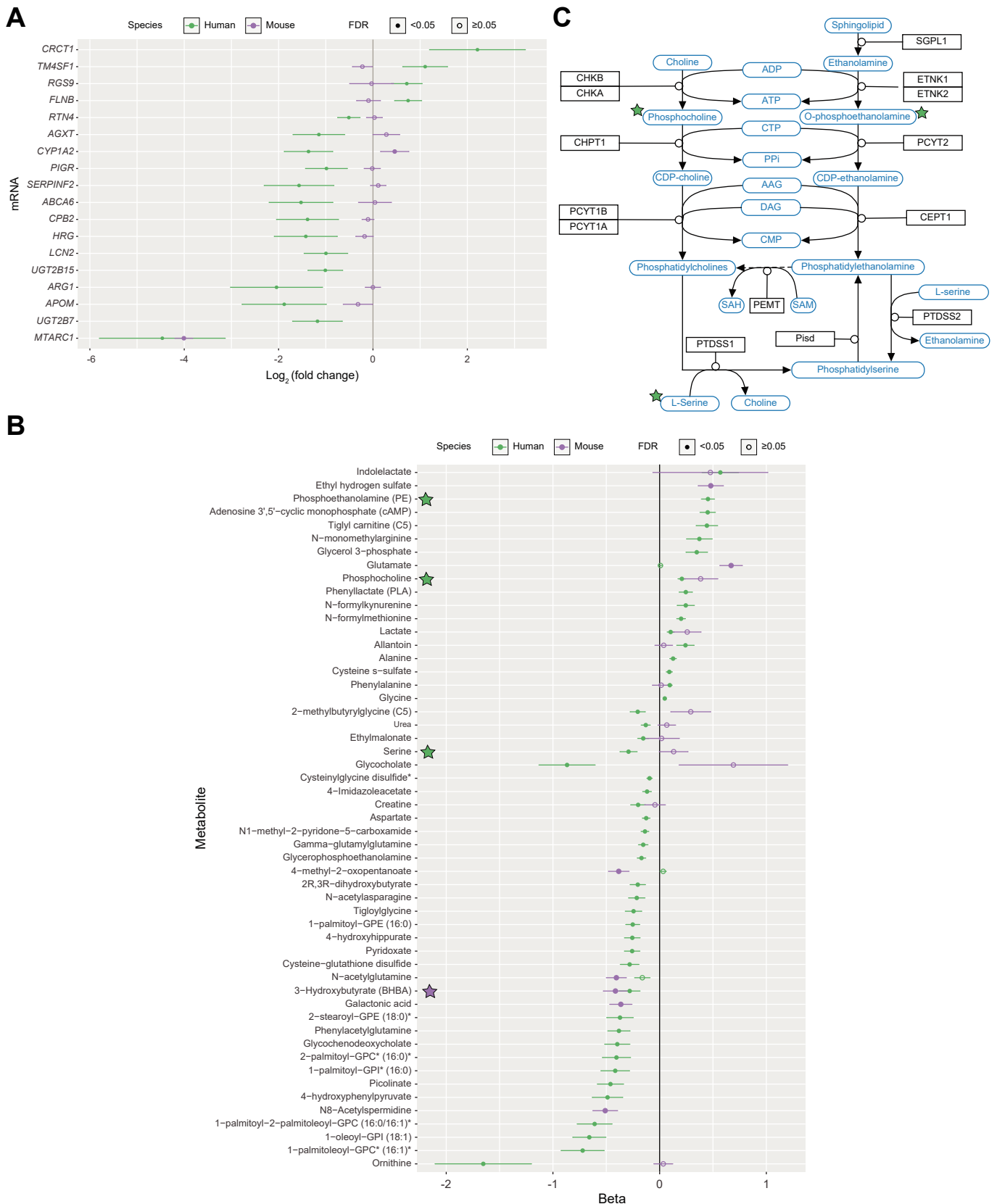


Fig. 5. Effect of *MTARC1* siRNA in PHH and mouse samples evaluated by omics approaches. (A) RNA sequencing data showing fold change of significantly dysregulated mRNAs and (B) metabolomic data showing significantly dysregulated metabolites in PHH (green) and mouse tissue from bulk liver prep (purple). FDR ≥ 0.05 (empty points) or FDR < 0.05 (solid points). 3-Hydroxybutyrate (purple star) was significantly reduced in both PHH and mouse samples. (C) Protein-interaction network analysis of significant metabolites revealed significant enrichment in the Kennedy pathway caused primarily by dysregulation of phosphocholine, phosphoethanolamine, and serine (green star). FDR, false discovery rate; *MTARC1*, mitochondrial amidoxime-reducing component 1; PHH, primary human hepatocytes.

The cell type(s) that mediate the effect of genetic variation in *MTARC1* on the various metabolic traits has important therapeutic implications. Beneficial effects of hepatocyte-specific *MTARC1* inhibition could be therapeutically tractable using GalNAc–siRNA technology. Although PHH are the gold standard model for metabolic modelling, their long-term utility is limited by rapid dedifferentiation *in vitro*. Using the recently described 5C protocol for long-term PHH culture,²³ we have shown that siRNA knockdown is effective and persistent in this model and lipid accumulation can be stimulated by exposure to an FFA mix and inhibited by knocking down *DGAT2*, which catalyses the last step of TG synthesis. si-*MTARC1* decreased lipid accumulation in both the absence and presence of the FFA mixture. The decreased lipid accumulation was not associated with alterations in FA uptake, as assessed by the remaining concentration observed in conditioned media, or oxidation of FA or DNL from glucose. GalNAc–si-*Mtarc1* treatment of Gubra DIO–NASH mice decreased hepatic TG content. PBS was used as a vehicle control rather than a GalNAc–NT siRNA owing to difficulties in assessing proper internalisation without an mRNA knockdown readout and the potential of off-target effects that may confound results. Although a contribution of the GalNAc moiety to the effects of GalNAc–si-*Mtarc1* treatment cannot be excluded, this concern is mitigated by concordant effects of si-*MTARC1* across model systems with independent siRNA delivery methods. Knockdown of hepatocyte mARC1 decreased neutral lipid content in PHH and mice, suggesting that hepatocyte *MTARC1* mediates the genetic associations with NAFLD. This has major therapeutic implications given the clinical utility of GalNAc conjugation to effectively deliver RNAi-based therapies to hepatocytes.

Hepatocytes secrete significant amounts of TG within VLDLs. As the anti-steatotic effect observed in carriers of the A allele of rs2642438 is accompanied by elevated plasma TG, increased VLDL secretion has been proposed as a potential mechanism by which *MTARC1* loss of function may reduce hepatic lipid content.⁸ Our findings that hepatocyte mARC1 knockdown increased supernatant and plasma TG in PHH and mice, respectively, support this hypothesis. Furthermore, the decreased secretion of apo B in PHH treated with si-*MTARC1* parallels decreased apo B in carriers of the A allele of rs2642438.^{3,8} This suggests that loss of hepatocyte

mARC1 function may decrease the number but increase the size of secreted VLDL particles, leading to reduced apo B and increased plasma TG, respectively. Transcriptomic analysis demonstrated a decreased expression of genes involved in FA metabolic processes and PPAR signalling upon mARC1 knockdown *in vitro* and *in vivo*. These findings are consistent with the decreased concentration of 3-hydroxybutyrate in cell culture supernatant and mouse plasma following mARC1 knockdown. Observed alterations in the Kennedy pathway in si-*MTARC1*-treated PHH are consistent with the observation that carriers of the A allele of rs2642438 have increased phosphatidylcholine in liver biopsies, which is essential for the secretion of VLDL.^{8,31} Together, these findings suggest that *MTARC1* inhibition influences TG secretion, rather than lipid catabolism, to reduce hepatic TG. The molecular mechanisms by which mARC1 exerts its effects on TG metabolism, and whether changes in 3-hydroxybutyrate and the Kennedy pathway are causative, require further study.

Although human genetics links *MTARC1* to more advanced forms of NAFLD,^{31–33} hepatocyte-specific knockdown of mARC1 did not improve previously established fibrosis in a DIO–NASH model. This may be attributable to a contribution of non-hepatocyte mARC1 to the genetic signal, species differences, or temporal considerations. The anti-steatotic effect of mARC1 inhibition may be sufficient to prevent, but not reverse, the development of fibrosis in agreement with a *Mtarc1*-induced reduction of α -SMA. Alternatively, a longer treatment period may be necessary to impact fibrosis in the DIO–NASH model. Future studies will be necessary to determine whether mARC1 alters fibrosis, whether such an effect is mediated via steatosis or direct mechanisms, and when in the disease progression therapeutic intervention may be effective.

In summary, genetically predicted *MTARC1* gene expression is associated with multiple metabolic traits, and hepatocyte mARC1 likely mediates the association with hepatic and plasma lipids. Knockdown of mARC1 in PHH and mice decreases intra-hepatocellular lipid content and increases TG secretion. This work supports the therapeutic utility of hepatocyte-specific targeting of mARC1 and further studies to elucidate the mechanisms by which mARC1 impacts NAFLD.

Abbreviations

5C, five chemicals; α -SMA, α -smooth muscle actin; ALP, alkaline phosphatase; ALT, alanine aminotransferase; apo A, apolipoprotein A; apo B, apolipoprotein B; AST, aspartate transaminase; DGAT2, Diacylglycerol O-acyltransferase 2; DNL, de novo lipogenesis; eQTL, expression quantitative trait locus; FA, fatty acid; FDR, false discovery rate; FFA, free fatty acid; GalNAc, N-acetylgalactosamine; GalNAc–si-*Mtarc1*, GalNAc-conjugated siRNA targeting murine *Mtarc1*; GAN, Gubra Amylin NASH; GWAS, genome-wide association studies; HyPrColoc, Hypothesis Prioritisation in multi-trait Colocalisation; IV, instrumental variable; IVW, inverse-variance weighting; MR, Mendelian randomisation; *MTARC1*, mitochondrial amidoxime-reducing component 1; NAFLD, non-alcoholic fatty liver disease; NASH, non-alcoholic steatohepatitis; PHH, primary human hepatocytes; PPAR, peroxisome proliferator-activated receptor; SHBG, Sex hormone binding globulin; si-*DGAT2*, siRNA targeting *DGAT2*; si-*MTARC1*, *MTARC1* targeting siRNA; siNT, non-targeting siRNA; TC, total cholesterol; TG, triglycerides.

Financial support

This work was supported by Novo Nordisk. SRN has a Novo Nordisk Postdoctoral Fellowship run in partnership with the University of Oxford and the British Heart Foundation (Fellowship FS/15/56/31645 and FS/SBSRF/21/31013 to LH).

Conflicts of interest

A provisional patent application directed to the subject matter disclosed in this manuscript has been filed by Novo Nordisk A/S. LCL, LC, LSH, RRK, CM, JN, CED, STH, RP, IS, EJJ, TND, AC, SH, BG, MEG, ETM, AHAE, WGH, KC, JF, JMMH, BA, and MAR are Novo Nordisk A/S or Novo Nordisk Ltd employees. EW and NWP are former Dicerna employees. SBR is a former employee of Dicerna Pharmaceuticals Inc. and presently employed by the Novartis Institutes for BioMedical Research (NIBR), Cambridge, MA, USA. WL is a former employee of Dicerna Pharmaceuticals and presently employed with Biogen Inc, Cambridge, MA, USA. LH is a scientific consultant for Novo Nordisk A/S. The remaining authors declare no competing interests.

Please refer to the accompanying ICMJE disclosure forms for further details.

Authors' contributions

Performed experiments and procedures: LCL, MAR, LSH, RP, EJJ, TND, IS, BG, AC, MEG, AHAE, CED, STH, JN, SRN, EW, SBR, WL. Contributed to concept and design of the study: LCL, MAR, CED, NWP, BA, STH, KC, JF, JMMH, WGH. Contributed to formal analysis and data curation: LCL, MAR, EJJ, TND, IS, CED, RRK, EMT, LC, CM, SH, NWP, BA, STH, JF, JN, SRN, EW, SBR, WL. Were involved in original draft preparation: LCL, MAR, CED, RRK,

LC, CM, JMMH, BA, STH, SRN. Supervised the study: MAR, BA, JMMH, LH, JF, KC. Reviewed and approved the final manuscript: all authors.

Data availability statement

The authors confirm that the data supporting the findings of this study are available within the article and Supplementary information. The transcriptomic and metabolomic datasets are available in GEO (GSE225616 for mouse and GSE223652 for human) and MetaboLights (MTBLS6909),³⁴ respectively.

Acknowledgements

The authors would like to thank T. Monfeuga, L. Payne, H.D. Radic, H. Lykkegaard, M.B. Larson, and M. Grønborg for their excellent technical support. P.S. Petersen and M. Feigh at Gubra Aps are acknowledged for study management and development of the biopsy-confirmed DIO NASH mouse model. M. Abrams, C. Rijnbrand, and M. McGrath are acknowledged for sourcing the work carried out by Dicerna Pharmaceuticals Inc. The authors gratefully acknowledge the UK Biobank and all the participants in the UK Biobank for providing data application #53639. The graphical abstract was created with BioRender.com.

Supplementary data

Supplementary data to this article can be found online at <https://doi.org/10.1016/j.jhepr.2023.100693>.

References

Author names in bold designate shared co-first authorship

- [1] Makri E, Goulas A, Polyzos SA. Epidemiology, pathogenesis, diagnosis and emerging treatment of nonalcoholic fatty liver disease. *Arch Med Res* 2021;52:25–37.
- [2] Mintziori G, Polyzos SA. Emerging and future therapies for nonalcoholic steatohepatitis in adults. *Expert Opin Pharmacother* 2016;17:1937–1946.
- [3] Emdin CA, Haas ME, Khera AV, Aragam K, Chaffin M, Klarin D, et al. A missense variant in mitochondrial amidoxime reducing component 1 gene and protection against liver disease. *PLOS Genet* 2020;16:e1008629.
- [4] **Innes H, Buch S**, Hutchinson S, Guha IN, Morling JR, Barnes E, et al. Genome-wide association study for alcohol-related cirrhosis identifies risk loci in *MARC1* and *HNRNPUL1*. *Gastroenterology* 2020;159:1276–1289.e1277.
- [5] Emdin CA, Haas M, Ajmera V, Simon TG, Homburger J, Neben C, et al. Association of genetic variation with cirrhosis: a multi-trait genome-wide association and gene–environment interaction study. *Gastroenterology* 2021;160:1620–1633.e1613.
- [6] **Haas ME, Pirruccello JP, Friedman SN**, Emdin CA, Ajmera VH, Simon TG, et al. Machine learning enables new insights into clinical significance of a genetic contribution to liver fat accumulation. *Cell Genom* 2021;1:100066.
- [7] Gao C, Marcketta A, Backman JD, O'Dushlaine C, Staples J, Ferreira MAR, et al. Genome-wide association analysis of serum alanine and aspartate aminotransferase, and the modifying effects of BMI in 388k European individuals. *Genet Epidemiol* 2021;45:664–681.
- [8] Schneider CV, Schneider KM, Conlon DM, Park J, Vujkovic M, Zandvakili I, et al. A genome-first approach to mortality and metabolic phenotypes in *MTARC1* p.Ala165Thr (rs2642438) heterozygotes and homozygotes. *Med (N Y)* 2021;2:851–863.e853.
- [9] **Vujkovic M, Ramdas S**, Lorenz KM, Guo X, Darlay R, Cordell HJ, et al. A multi-ancestry genome-wide association study of unexplained chronic ALT elevation as a proxy for nonalcoholic fatty liver disease with histological and radiological validation. *Nat Genet* 2022;54:761–771. <https://doi.org/10.1038/s41588-022-01078-z>.
- [10] Anstee QM, Darlay R, Cockell S, Meroni M, Govaere O, Tiniakos D, et al. Genome-wide association study of non-alcoholic fatty liver and steatohepatitis in a histologically characterised cohort. *J Hepatol* 2020;73:505–515.
- [11] Fairfield CJ, Drake TM, Pius R, Bretherick AD, Campbell A, Clark DW, et al. Genome-wide association study of NAFLD using electronic health records. *Hepatol Commun* 2022;6:297–308.
- [12] Klein JM, Busch JD, Potting C, Baker MJ, Langer T, Schwarz G. The mitochondrial amidoxime-reducing component (*mARC1*) is a novel signal-anchored protein of the outer mitochondrial membrane. *J Biol Chem* 2012;287:42795–42803.
- [13] Kubitzka C, Bittner F, Ginsel C, Havemeyer A, Clement B, Scheidig AJ. Crystal structure of human *mARC1* reveals its exceptional position among eukaryotic molybdenum enzymes. *Proc Natl Acad Sci U S A* 2018;115:11958–11963.
- [14] Sparacino-Watkins CE, Tejero J, Sun B, Gauthier MC, Thomas J, Ragireddy V, et al. Nitrite reductase and nitric-oxide synthase activity of the mitochondrial molybdopterin enzymes *mARC1* and *mARC2*. *J Biol Chem* 2014;289:10345–10358.
- [15] Ott G, Havemeyer A, Clement B. The mammalian molybdenum enzymes of *mARC*. *J Biol Inorg Chem* 2015;20:265–275.
- [16] Havemeyer A, Lang J, Clement B. The fourth mammalian molybdenum enzyme *mARC*: current state of research. *Drug Metab Rev* 2011;43:524–539.
- [17] Jakobs HH, Mikula M, Havemeyer A, Strzalkowska A, Borowa-Chmielak M, Dzwonek A, et al. The N-reductive system composed of mitochondrial amidoxime reducing component (*mARC*), cytochrome b5 (*CYB5B*) and cytochrome b5 reductase (*CYB5R*) is regulated by fasting and high fat diet in mice. *PLoS One* 2014;9:e105371.
- [18] Neve EP, Köfeler H, Hendriks DF, Nordling A, Gogvadze V, Mkrtchian S, et al. Expression and function of *mARC*: roles in lipogenesis and metabolic activation of ximelagatran. *PLoS One* 2015;10:e0138487.
- [19] Rixen S, Havemeyer A, Tyl-Bielicka A, Pysiak K, Gajewska M, Kulecka M, et al. Mitochondrial amidoxime-reducing component 2 (*MARC2*) has a significant role in N-reductive activity and energy metabolism. *J Biol Chem* 2019;294:17593–17602.
- [20] Neve EP, Nordling A, Andersson TB, Hellman U, Diczfalusy U, Johansson I, et al. Amidoxime reductase system containing cytochrome b5 type B (*CYB5B*) and *MOSC2* is of importance for lipid synthesis in adipocyte mitochondria. *J Biol Chem* 2012;287:6307–6317.
- [21] Bycroft C, Freeman C, Petkova D, Band G, Elliott LT, Sharp K, et al. The UK Biobank resource with deep phenotyping and genomic data. *Nature* 2018;562:203–209.
- [22] Van Hout CV, Tachmazidou I, Backman JD, Hoffman JD, Liu D, Pandey AK, et al. Exome sequencing and characterization of 49,960 individuals in the UK Biobank. *Nature* 2020;586:749–756.
- [23] **Xiang C, Du Y, Meng G**, Soon Yi L, Sun S, Song N, et al. Long-term functional maintenance of primary human hepatocytes in vitro. *Science* 2019;364:399–402.
- [24] Diaz G, Melis M, Batetta B, Angius F, Falchi AM. Hydrophobic characterization of intracellular lipids in situ by Nile Red red/yellow emission ratio. *Micron* 2008;39:819–824.
- [25] Evans AM, Bridgewater B, Liu Q, Mitchell MW, Robinson RJ, Dai H, et al. High resolution mass spectrometry improves data quantity and quality as compared to unit mass resolution mass spectrometry in high-throughput profiling metabolomics. *Metabolomics* 2014;4:2. <https://doi.org/10.4172/2153-0769.1000132>.
- [26] Doneanu CE, Chen WM, Mazzeo JR. UPLC/MS monitoring of water-soluble vitamin Bs in cell culture media in minutes. Milford, MA, U.S.: Waters Corporation; 2011. Report No. 720004042en.
- [27] Foley CN, Staley JR, Breen PG, Sun BB, Kirk PDW, Burgess S, et al. A fast and efficient colocalization algorithm for identifying shared genetic risk factors across multiple traits. *Nat Commun* 2021;12:764.
- [28] Mathieson T, Franken H, Kosinski J, Kurzawa N, Zinn N, Sweetman G, et al. Systematic analysis of protein turnover in primary cells. *Nat Commun* 2018;9:689.
- [29] Allende DS, Gawrieh S, Cummings OW, Belt P, Wilson L, Van Natta M, et al. Glycogenosis is common in nonalcoholic fatty liver disease and is independently associated with ballooning, but lower steatosis and lower fibrosis. *Liver Int* 2021;41:996–1011.
- [30] Struwe MA, Clement B, Scheidig A. Letter to the editor: the clinically relevant *MTARC1* p.Ala165Thr variant impacts neither the fold nor active site architecture of the human *mARC1* protein. *Hepatol Commun* 2022;6:3277–3278.
- [31] Luukkonen PK, Juuti A, Sammalkorpi H, Penttilä AK, Orešič M, Hyötyläinen T, et al. *MARC1* variant rs2642438 increases hepatic phosphatidylcholines and decreases severity of non-alcoholic fatty liver disease in humans. *J Hepatol* 2020;73:725–726.
- [32] **Mann JP, Pietzner M**, Wittemans LB, Rolfe EL, Kerrison ND, Imamura F, et al. Insights into genetic variants associated with NASH–fibrosis from metabolite profiling. *Hum Mol Genet* 2020;29:3451–3463.
- [33] Hudert CA, Adams LA, Alisi A, Anstee QM, Crudele A, Draijer LG, et al. Variants in mitochondrial amidoxime reducing component 1 and hydroxysteroid 17-beta dehydrogenase 13 reduce severity of nonalcoholic fatty liver disease in children and suppress fibrotic pathways through distinct mechanisms. *Hepatol Commun* 2022;6(8):1934–1948. <https://doi.org/10.1002/hep4.1955>.
- [34] Haug K, Cochrane K, Nainala VC, Williams M, Chang J, Jayaseelan KV, et al. MetaboLights: a resource evolving in response to the needs of its scientific community. *Nucleic Acids Res* 2020;48:D440–D444.